OSR: Advancing Multi-Hop Routing for LoRaWAN Mesh Networks in Maritime Scenarios

Salah Eddine Elgharbi*†, Mauricio Iturralde†, Yohan Dupuis† and Alain Gaugue*
*L3i, La Rochelle Université
†CESI LINEACT, CESI École d'Ingénieurs
salah-eddine.elgharbi@univ-lr.fr, miturralde@cesi.fr, ydupuis@cesi.fr, alain.gaugue@univ-lr.fr

***Abstract*—Reliable data acquisition and transmission from ocean-deployed buoys are crucial for maritime applications. However, wireless data transmission in such contexts faces significant challenges due to limited buoy battery capacity, harsh weather conditions, and potential disruptions from maritime vessels. LoRaWAN technology presents a promising solution due to its low power consumption and long-range communication capabilities. Multi-hop routing can further enhance network efficiency by enabling data relaying between buoys. However, the standard LoRaWAN framework lacks native support for multi-hop routing. Addressing this limitation, this paper presents a novel multi-hop routing protocol called OSR specifically designed for LoRaWAN mesh networks deployed in maritime environments. The protocol's effectiveness is evaluated through a simulation model that accurately reflects the detrimental effects of severe weather on data transmission. Key performance metrics, such as packet delivery ratio, end-to-end latency, and energy consumption are analysed. The results underscore the superiority of OSR over the conventional GRP under realistic marine channel conditions.**

***Index Terms*—Mesh network, LoRaWAN, Multi-hop opportunistic networking, Simulation**

I. Introduction

With the continuous growth of the Internet of Things (IoT), the number of IoT applications and deployments is expanding across various industries. Sectors such as maritime traffic management, port operations, and environmental monitoring are heavily reliant on these data [1]. Data collection is achieved through the strategic deployment of sensors in designated maritime locations. These raw data necessitate subsequent processing and analysis to yield actionable intelligence for informed decision-making. Buoys are commonly employed as platforms for sensor installation, facilitating data capture. Marine environments lack a consistent power supply and wired connections, necessitating wireless data transmission to onshore facilities. Consequently, optimising battery power is crucial for uninterrupted sensor network operation.

Maritime data transmission faces a further challenge due to the dynamic and often severe meteorological conditions, including significant wave action, storms, and precipitation. These factors can induce antenna motion, compromising the quality of the transmission link. The movement experienced during such conditions frequently leads to substantial packet loss. The deployment of buoys at significant distances offshore necessitates the adoption of a technology capable of long-range data transmission. In this context, Long Range Wide Area Networks (LoRaWAN) presents itself as a suitable solution due to its theoretical transmission range of up to 15 kilometres in unobstructed environments. However, as previously established, this range exhibits a pronounced susceptibility to degradation under the variable conditions encountered in maritime environments. The reliance on direct communication links between LoRa nodes and gateways becomes vulnerable to interference in environments susceptible to rapid changes [2]. Mitigating this challenge can be achieved through the implementation of a multi-hop routing protocol for packet delivery to the gateway with opportunistic multipath decisions. However, the standard LoRaWAN protocol inherently lacks native support for routing functionalities [3], rendering multi-hop packet forwarding infeasible in its unmodified state. Building upon our prior research that demonstrated the potential of a single-hop relay within LoRaWAN for maritime communication reliability up to three times compared to direct transmission [4], this paper presents a novel multi-hop routing protocol called Opportunistic Smart Routing (OSR), specifically designed for LoRaWAN deployments in maritime environments. The proposed mechanism was subjected to performance evaluation under a Realistic Channel Model (RCM) simulation incorporating severe meteorological conditions, accurately reflecting the antenna motion induced by such challenging scenarios. To evaluate the effectiveness of the proposed routing protocol, a comparative analysis is conducted against the conventional Geographic Routing Protocol (GRP) strategy in both its greedy and perimeter operational modes.

The structure of the remaining sections of this paper is organised as follows: Section II reviews relevant literature, critically examining current research in this field. Section III delves into the network architecture employed in the maritime scenario and the proposed routing methodology, detailing its features and implementation. Section IV describes the simulation environment, outlining its parameters and the benchmark algorithms used for performance evaluation. Section V analyses the results, emphasising significant findings. Finally, Section VI summarises the main findings and outlines potential avenues for further investigation.

II. Previous Works

The growing interest in LoRaWAN for maritime communication applications necessitates reliable and efficient data transmission over extended ranges. Existing multi-hop pro-

978-3-903176-66-9

tocols often lack adaptations for maritime challenges like dynamic topologies and complex signal propagation. This critical gap hinders the full potential of LoRaWAN in maritime communication. Several studies have proposed novel or modified Long Range (LoRa) mesh protocols, including Destination-Sequenced Distance-Vector routing (DSDV) [5], Routing Protocol for Low-Power and Lossy Networks (RPL) [6], and Ad-hoc On-Demand Distance Vector (AODV) [7]. However, despite advancements in maritime communication, multi-hop routing protocols specifically designed for LoRaWAN mesh networks remain scarce.

A self-organising maritime mesh network utilising white space routers deployed on buoys is proposed in [8]. The authors conducted tests over a 500 m range with antennas positioned at 5 m height and a transmission power of 25 dBm. Based on these test results, simulations predicted a achievable range of 5 km for a 2 Mbps signal at a transmission power of 30 dBm, with a RSSI of -85 dBm. However, it focuses on direct communication and lacks routing protocols. A Delay Tolerant Networking (DTN) protocol with sleep states for end-nodes in LoRa-based maritime communication to minimise power consumption is introduced in [9], acknowledging the trade-off with Packet Delivery Ratio (PDR). It investigates the impact of sleep state duration and communication distance on PDR to guide power-saving configuration in real-world deployments. A study by [10] explores a dual-layered LoRa mesh architecture for ship-to-ship communication. This architecture enables data exchange between vessels with a range of up to 5 km. However, the work identifies trade-offs between range and performance, including extended recovery times and high packet loss at greater distances. It also highlights the need for further investigation into latency and power consumption. LoRaBlink [11] proposes a multi-hop LoRa protocol for low-density networks with limited nodes. Integrated into the MAC layer, it uses time synchronisation for slotted channel access. While achieving reliable and energy-efficient communication, the flooding mechanism employed for connection establishment can be energy-intensive. Building upon DSDV [5], [12] proposes a simplified multi-hop LoRaWAN uplink extension. It categorises nodes as Leaf Nodes (LNs) and Relay Nodes (RNs) for routing table maintenance. Gateways (GWs) and RNs propagate routing information via beacons. LNs forward packets with routing overhead towards the path with the fewest hops, achieving good throughput and Packet Reception Ratio (PRR). However, hop count remains the sole route selection criterion. A study explores a synchronous LoRa-Mesh protocol for reliable data collection from Wireless Unfriendly Zones (WUZs) [13]. A RN maintains communication with a GW and establishes a tree structure with WUZs nodes. The RN synchronously gathers data in dedicated time slots and transmits it to the GW. Evaluations conducted at a distance of 1830 m revealed an energy consumption of 370 mJ. This value is expected to increase with the addition of new branches to the tree. Building upon RPL [6], a study proposes RLMAC for improved multi-hop communication in LoRa networks. It establishes a Directed Acyclic Graph (DAG) for upward/downward routing using distance-vector selection. A two-stage process with neighbour discovery determines optimal Spreading Factors. While RLMAC achieves high PDR (up to 86%), limitations exist: timing issues with Destination Oriented Directed Acyclic Graph Information Object (DIO) messages and a restricted scope (small network, limited testing). LoRaOpp [14] introduces a multi-hop protocol for intermittent LoRa networks. It defines end-nodes, peer-nodes, and gateways. Peer-nodes relay data using hop count or delay metrics. Gateways buffer packets for unreachable nodes. End-nodes advertise locally, while peer-nodes perform multi-hop broadcasts. The protocol adapts transmission based on channel conditions. Compared to the Epidemic Routing (ER) protocol, LoRaOpp might benefit from multiple gateways for enhanced packet delivery due to limited range. The research presented in [15] proposes a layered routing protocol for hierarchical networks. It employs energy-saving mechanisms: modifying routing messages and powering down end-nodes. Additionally, it balances network load. While outperforming AODV [7] in energy efficiency and delay, its effectiveness diminishes with frequent transmissions. The study's simplified model may not reflect real-world IoT environment interference.

Research on multi-hop routing in LoRaWAN networks has shown promise, but existing protocols often lack adaptations for maritime environments. This gap presents an opportunity to develop and evaluate routing protocols tailored to maritime LoRaWAN, addressing unique challenges like signal propagation and dynamic topologies through multi-hop strategies.

III. OPPORTUNISTIC SMART ROUTING

Initially, a novel Decentralised LoRaWAN Mesh Network (DLM) network architecture, specifically designed for maritime applications, is introduced. The DLM network topology comprises four distinct node types denoted by N_t:

- End Device (ED): transmits the harvested data from the IoTs to RLs, RRs, or directly to GWs.
- Relay Device (RL): receives data from EDs and RRs and performs single-hop forwarding to GWs.
- Router Device (RR): possesses multi-hop routing capabilities, receiving data from EDs and forwarding packets to other RRs or RLs.
- Gateway (GW): solely receives packets from EDs or RLs and forwards them to the cloud infrastructure LoRaWAN servers.

The DLM network's suitability for ED deployments stems from the OSR protocol, as shown in Fig. 1. The proposed architecture positions each buoy at a designated location offshore. These buoys are equipped with LoRa sensors to acquire and monitor oceanic data. However, mobile vessels or waves can intermittently disrupt the line-of-sight radio links between buoys and the GW, increasing packet loss and degrading connection quality.

A. The OSR protocol

The OSR algorithm employs a dynamic, tree-based approach within network neighbourhoods to optimise routing

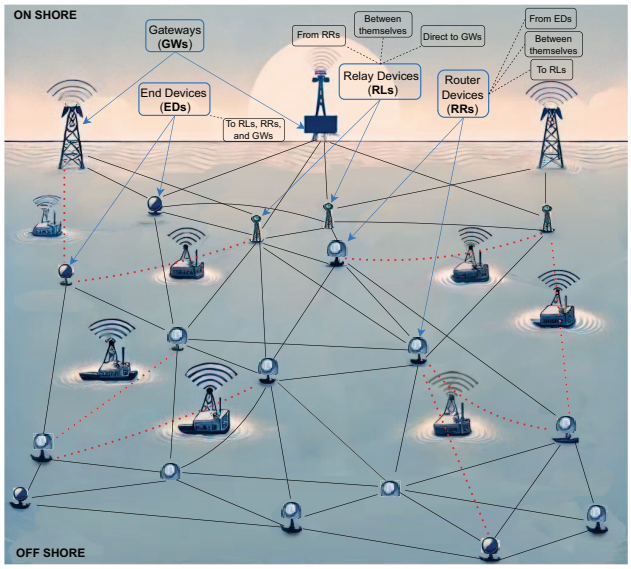

Fig. 1: Network topology adopted for DLM application.

decisions in the DLM network. This optimisation is achieved by selecting the most efficient path based on real-time assessments of network conditions. The algorithm leverages a cross-layer design principle [16], integrating LoRa/LoRaWAN with established hybrid techniques [17]. This integration facilitates the selection of a balanced set of routing metrics within the OSR framework. The core objective function prioritises a combination of two key factors: finding the optimal path based on current link state information and selecting a short path for efficient routing. This combined approach fosters a scalable and efficient routing strategy by optimising transmission performance and mitigating the negative impacts of signal shadowing effects.

We subsequently present a simplified mathematical foundation for OSR, detailing the computations and processing involved in its routing decisions. Following successful authentication, the OSR mechanism is activated for each node N within the set $\{ED, RL, RR, GW\}$. This activation process initiates communication with adjacent neighbours. Any changes in network topology or packet transmissions will subsequently affect the intermediate mesh nodes (collectively denoted as $RD = RL \cup RR$), as described in the initial section of the OSR-DLM processing Algorithm 1. The OSR algorithm initiates by evaluating the network state for transmission, encompassing the occupied LoRa channel (three-channel used Ch_c: Ch_1, Ch_2, or Ch_3) and network parameters N_p like node positions, neighbour information, standby mode, spreading factor, bandwidth, payload size, and coding rate. Additionally, it considers node rankings mode used R_k relevant to different N_t. Following this assessment, each node in the DLM network periodically transmits a prediction packet (acting as a beacon) at predefined intervals (T, default: every 40 seconds) to identify and scan potential subroutes r^* among neighbours as outlined in Eq. 1. Furthermore, this process

Algorithm 1 RD Node Routing Packet Processing.

```
procedure OSR-DLM()
    CheckIfKnownNeighbor ← KnownNeighbor(P)
    if CheckIfKnownNeighbor then
        UpdateEntryTable(P)
        CheckIfPacketContainRoutes ← ContainRoutes(P)
        if CheckIfPacketContainRoutes then
            ProcessNextRoute()
            CheckIfKnownRoute ← KnownRoute(P)
            if CheckIfKnownRoute then
                UpdateMetrics(P)
                OSR(P)                          ▷ Path and rank selection
                ProcessUnprocessedRoute()
            else
                AddNodeAndRoute()
            end if
        else
            DeletePacket(P)
        end if
    else
        AddAsNewNeighbour()
    end if
end procedure
```

assesses and updates the current state of the DLM network. This process serves a dual purpose: 1) proactively updating OSR metrics in the routing table based on anticipated changes in link quality (via Signal-to-Noise Ratio (SNR) and Received Signal Strength Indication (RSSI)) or network topology, and 2) triggering low power mode (LP) activation for energy conservation by adjusting the operational state (sleep/wake-up) of other nodes, as encapsulated by the equation:

$$r^* \leftarrow \text{CheckState}(N_p, N_t, LP, t) \quad \forall N_t \in N, t \in \mathbb{T}, \qquad (1)$$

where t represents individual evaluation intervals and $\mathbb{T}$ signifies the entire set of intervals highlighting OSR's continuous operation.

This predictive mechanism empowers nodes with autonomous decision-making capabilities. Nodes can proactively route transmissions around potential communication issues with other nodes in the mesh network, thereby mitigating the risk of collision time for Concurrent Transmission (CT) problems. This approach aligns well with the low-power Class A LoRaWAN deployment, minimising baseline energy consumption. However, in a large-scale DLM network, the computational framework remains alert, constantly evaluating whether to transition individual nodes into sleep or wake-up modes. While beneficial for overall network efficiency, disseminating these control signals inevitably increases energy expenditure across the system. A core aspect of the algorithm is the determination of the most suitable operational mode, denoted by M. This mode is determined based on network parameters N_p, node type N_t, and the predicted subroute r^* using the following equation:

$$M \leftarrow \text{DLMAdaptiveMode}(N_p, N_t, r^*), \qquad (2)$$

where the variable M can take on three values: 'Relay', 'Router'or 'Standard'. Each value dictates the specific packet routing methodology employed within the network, dynamically adapting to current network conditions. This adaptive approach optimises packet forwarding strategies, considering both network congestion and energy utilisation. Ultimately,

this ensures the continued integrity and efficacy of network communications. An important part of the OSR framework's adaptive decision-making process lies in the computation of a balanced metric selection ϕ for each potential subroute r^* (see Eq. 4). This metric is influenced by network parameters N_p, node types N_t, and node rankings R_k. Calculating ϕ is essential for determining the most efficient routing path from the source node S to the destination node D for a specific data packet P. This process culminates in the selection of the optimal nodes RD_z that constitute the best path, represented as $\varphi^* : \{S \Rightarrow RD_z \Rightarrow D\}$. Although the usual routing protocol will choose a less costly path, it depends on the channel state used (Ch_c). Transmission between neighbours using the same channel; moreover, the OSR algorithm employs a comprehensive objective function ψ to choose a lower-cost path base channel used as outlined in Eq. 3.

$$\min \psi(P) = \sum_{i=1}^{n-m} \phi(\mathrm{d}_i, \mathrm{T}_{\mathrm{art}_i}, H_{\mathrm{DLM}}(\mathrm{s,d})_i, \mathrm{RxPw}(Ch_c)_i) \quad \forall md \in M, \quad (3)$$

where $c = 1, 2, 3$. Equation 3 incorporates a balanced metric selection function ϕ, defined in Eq. 4. Within this context: n specifies the total number of nodes in the DLM network, m the number of GW nodes, and ϕ optimises various factors including shortest distance d, minimal airtime $\mathrm{T}_{\mathrm{art}}$, least number of hops (derived from the network distance, $H_{DLM}(s, d)$), and optimal received signal strength (RxPw) using Spreading Factor 7 (SF7). This configuration targets a Signal-to-Noise Ratio (SNR) of -7.5 dB and a Received Signal Strength Indicator (RSSI) of -129.995 dBm, facilitating the detection of severe weather conditions for the buoys used and temporary link outages caused by vessels. For different modes, the node rankings R_k, are determined based on the specific selection of weighting ϕ, as illustrated in the following equation:

$$\phi = \begin{cases} \phi_{\mathbf{1}} & \text{for} \quad N_t\colon ED, GW \quad R_k\colon 0 \\ \phi_{\mathbf{2}} & \text{for} \quad N_t\colon ED, RL, GW \quad R_k\colon 1 \\ \phi_{\mathbf{3}} & \text{for} \quad N_t\colon ED, RL, RR, GW \quad R_k\colon z, z > 2, \end{cases} \quad (4)$$

$\phi_{\mathbf{1}}$ for direct neighbours of the GW, $\phi_{\mathbf{2}}$ for nodes two hops away from the GW, and $\phi_{\mathbf{3}}$ for nodes n hops away from the GW. The variable N_t refers to the device type participating in forwarding. This distributed approach fosters the creation of a decentralised mesh network architecture with multiple path selection options.

The DLM network leverages Device to Device (D2D) communication for mesh crowd sourcing, optimising routing decisions. The previously analysed objective function, $\psi(P)$ (see Eq. 3), facilitates the identification of a comprehensive set of potential optimal paths φ^*. These paths are represented as a tree-based path to optimize routing decisions: φ^*: $(\psi(P) = \{\varphi_1, \varphi_2, \ldots, \varphi_n\})$, where each φ_i signifies an optimal route. The identified paths are then ordered by cost-effectiveness, prioritising routes with the fewest hops. This directly addresses collision time concerns as fewer hops reduce CT. This methodology remains applicable in scenarios with multiple gateways. Following the selection of the most efficient route (e.g., φ_1) and the determination of the operational mode M, the packet is prepared for transmission. The process involves sending and receiving the packet along the chosen path.

The OSR algorithm continuously monitors and adjusts routing parameters and the network state to maintain synchronisation. Building upon the foundation laid out for EDs, RRs exhibit more complex behaviour. While the core packet processing protocol remains similar, RRs introduce modifications during the encapsulation and decapsulation phases to accommodate routing functionalities. Crucially, RRs leverage a sophisticated routing mechanism. They comprehensively evaluate all available routing entries within their tables using the ϕ function (see Eq. 4). This mechanism facilitates the identification of the optimal route for packet forwarding, ensuring efficient data delivery throughout the network. RLs prioritise speed and efficiency. They serve a straightforward function: relaying packets towards the nearest accessible gateway. This approach [4], expedites transmission and minimises delays, optimising network performance.

B. The OSR Packet structure

OSR priorities bandwidth efficiency by employing a shared packet structure (see Fig. 2) for data and routing information and taking advantage of unused fields such as reserved for future use (RFU) in the standard LoRaWAN packet, we adhere to the LoRaWAN standard structure with some modifications. We propose a new packet structure which minimises header overhead (typically $n + 7$ bytes), crucial for accommodating OSR protocols within LoRa's 256-byte payload limit. Key fields include 2-byte source/destination identifiers, an optional 2-byte next-hop field (updated by intermediary nodes), a 1-byte flag with 3-bit RFU and 5-bit Time-To-Live (TTL), and a flexible payload for application data or routing information (maximum size: m bytes based on region, data rate, and spreading factor).

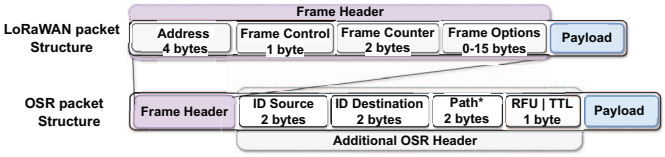

Fig. 2: OSR packet structure.

IV. Experimental Framework

This section outlines the simulation environment employed to evaluate the performance of our proposed routing model. We describe the network topology, deployment scenarios, configuration settings, physical model, key performance indicators, and comparative analysis against GRP variants GRP-Greedy (GRP-G) and GRP-Perimeter (GRP-P). These variants, renowned for their ability to navigate dynamic network complexities through optimized packet forwarding [18], [19], were selected due to their similarity to OSR.

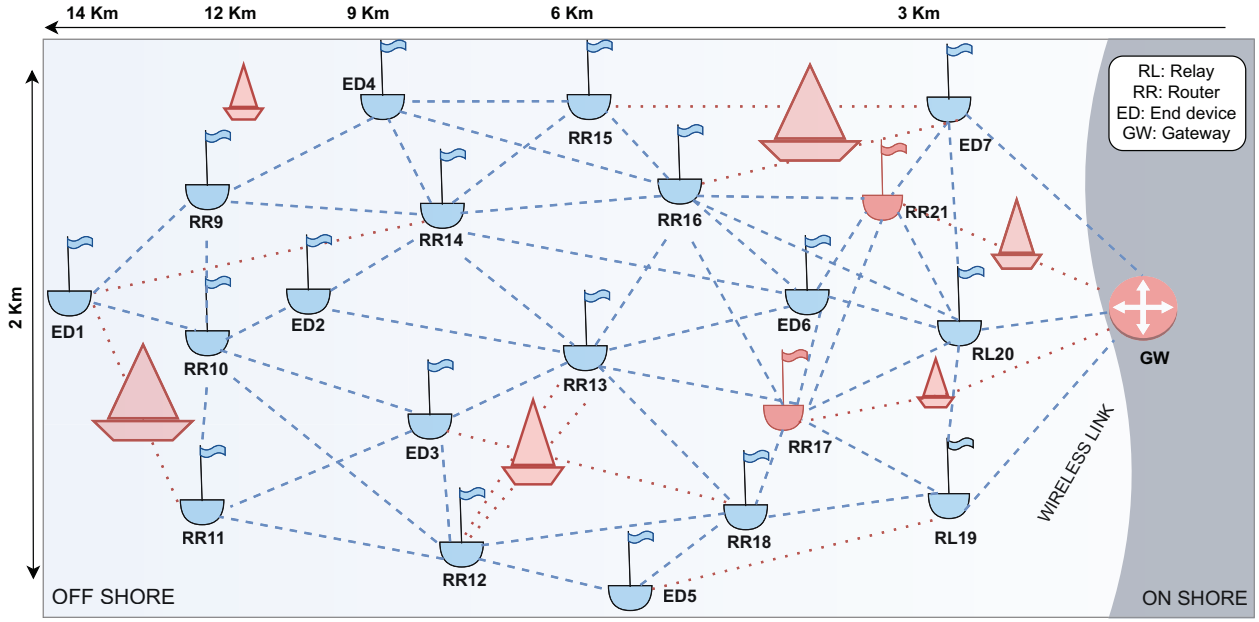

Fig. 3: Spatial distribution of the buoy-based DLM network. Red lines indicate LoRaWAN radio links with significant degradation due to vessel interference or sensitivity issues, while blue lines represent links with superior radio quality.

A. Simulation tool

We leverage the well-established discrete-event network simulator, ns-3 [20], to evaluate our OSR model's performance. Table I summarises the key configuration parameters employed within the simulation.

Parameter	Value
Frequency	433 MHz
Bandwidth	125 KHz
Coding rate	4/5
Transmission power	14 dBm
SF (Spreading Factor)	7
Coding rate	4/5
Packet size	23 Bytes
Preamble length	8
Duty Cycle	1%
Number of nodes	21
Covered areas	14000 m x 2000 m
Packet interval	100 s
Shadowing parameter (RCM)	True

TABLE I: Simulation parameters.

The simulation scenario evaluates the OSR framework in a maritime network with 21 nodes (1 gateway, 7 End Devices, 11 Relay Routers, and 2 Relay Links) deployed along a 14-kilometre coastal stretch. Nodes were randomly positioned to ensure logical connectivity. The distances between each ED and the gateway are: ED1 (13.91 km), ED2 (9.01 km), ED3 (8.54 km), ED4 (8.60 km), ED5 (6.52 km), ED6 (4.92 km), and ED7 (1.89 km). A five-hour simulation was conducted with EDs transmitting 23-byte payloads every 100 seconds. Each experiment was repeated 25 times, and results were averaged with variance included to illustrate the distribution of outcomes.

B. Physical Model

A maritime-specific physical model is employed to simulate signal propagation [4]. This model incorporates the influence of environmental factors such as sea and air temperature, as well as sea surface roughness, on wave propagation. To simulate attenuation in ns-3, we employed a modified log-distance power law for path loss calculations in LoRa transmissions, expressed in dB as:

$$\text{Att}(\text{txPwDbm}, d) = -X(d_0) - 10n \log\left(\frac{d}{d_0}\right) + S_{\text{dt}}, \quad (5)$$

where d_0 denotes the distance between the receiver and transmitter, measured in meters, n represents the path loss exponent, $X(d_0)$ indicates the path loss observed at a reference distance, txPwDbm represents the transmission power predicated by our maritime specific physical model, and the RCM testbed employs a deterministic shadowing loss model (S_{dt}) to represent attenuation shadowing effects based on the specific configuration of obstacles (e.g., boats).

C. Quality of Service parameters

We analyse the following key Quality of Service (QoS) parameters:

1) Packet Delivery Ratio (PDR): This parameter is defined as the ratio of successfully received γ and decoded packets at the gateway to the total number transmitted δ by EDs. The PDR is mathematically expressed as:

$$\text{PDR} = \frac{\gamma}{\delta} \times 100, \quad (6)$$

2) End-to-End Latency: This parameter reflects the total packet travel time from source to destination. It is the average one-way delay across hops, calculated as the difference between the transmission timestamp T_S at the source and the reception timestamp T_R at the destination (see Eq. 7).

$$\text{Latency} = T_R - T_S, \tag{7}$$

3) Energy Consumption Model: Energy consumption E_{con} is a critical metric for assessing network longevity. It is calculated by subtracting the remaining energy R_{energy} from the initial battery capacity EI_{energy}. The energy consumption for various operational modes (M) involved in transmission is as follows:

$$\begin{aligned} E_{\text{con}} &= E_{\text{Active}} + E_{\text{Sleep}}, \\ E_{\text{Active}} &= \alpha \cdot t_{\text{tx}} + \beta \cdot t_{\text{rx}} + \theta \cdot t_{\text{standby}}, \\ E_{\text{Sleep}} &= \omega \cdot t_{\text{sleep}}, \end{aligned} \tag{8}$$

where α, β, θ, and ω are coefficients representing energy consumption rates in transmit, receive, standby, and sleep states, respectively, with their durations t_{tx}, t_{rx}, t_{standby}, and t_{sleep} for each participating RD_z nodes during forwarding.

V. Results and Analysis

This section presents the experimental results and analysis. We benchmarked the proposed OSR protocol against established GRP variants to evaluate its performance.

Fig. 4 shows the PDR for each device transmitting to the gateway. OSR consistently outperforms both GRP-Greedy and GRP-Perimeter at all distances.

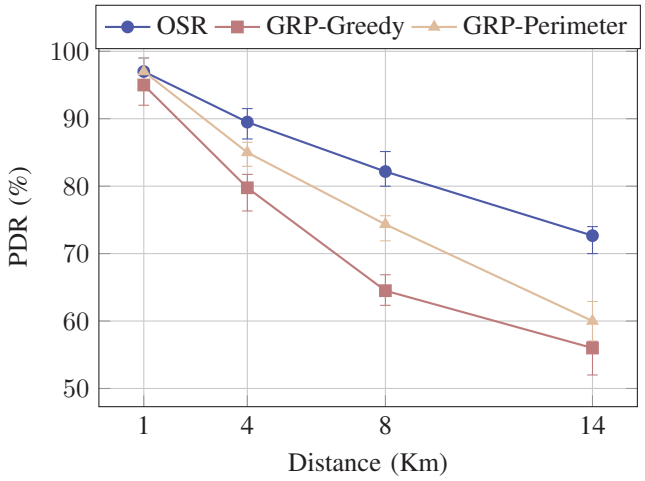

Fig. 4: Packet delivery ratio.

At close proximity (1 km), OSR and GRP-P achieve similarly high PDR 97%. This behaviour can be attributed to the effectiveness of direct communication or a single-hop relay in scenarios with minimal signal obstruction. At greater distances, OSR's performance advantage becomes evident. At (4 km), OSR maintains a 90% PDR compared to 85% and 80% for GRP-P and GRP-G, respectively. At (8 km), OSR scores 83%, while GRP-Perimeter and GRP-Greedy score 74% and 64%, respectively. At (14 km), the scores are 74% for OSR, 60% for GRP-Perimeter, and 57% for GRP-Greedy. The gap between OSR and the GRP variants increases with distance. OSR's superior performance is attributed to its multi-path selection, loop-free routing, and adaptability to dynamic environments. Unlike GRP algorithms, which rely solely on node positions, OSR constructs balanced routing strategies based on the network topology, resulting in lower hop ratios and extended connectivity with fewer relay points. GRP-G nearest neighbor strategy introduces additional hops, increasing communication load and reducing efficiency. While GRP-P perimeter-based planar graph routing is better suited for obstacle avoidance, OSR adaptability in WUMZ conditions optimizes delivery by dynamically selecting between direct transmission, single-hop forwarding, or multi-hop routing.

Fig. 5 depicts end-to-end latency variations for devices at distances of 1 km, 4 km, 8 km, and 14 km from the gateway.

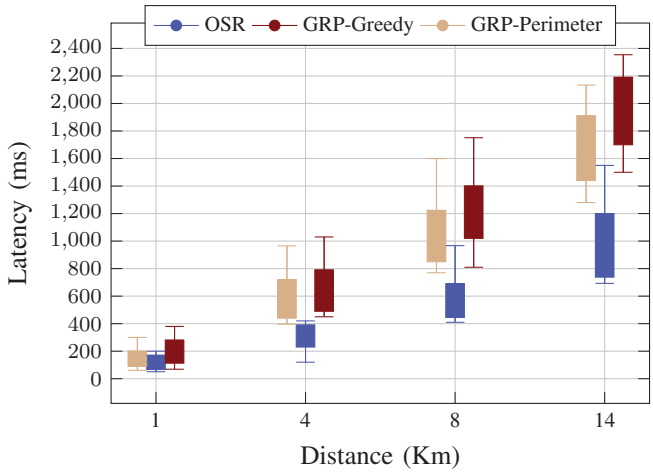

Fig. 5: Boxplot depicting the impact of gateway distance on end-to-end latency distribution for EDs.

At (1 km), simple routes result in similar latencies for all protocols. OSR latencies range from 51 ms to 200 ms, lower than GRP-Greedy's 69 ms to 380 ms and GRP-Perimeter's 61 ms to 300 ms. At (4 km), OSR exhibits lower latency (min: 120 ms - max: 420 ms) compared to GRP-G (min: 450 ms - max: 1030 ms) and GRP-P (min: 396 ms - max: 965 ms). This observed disparity in end-to-end delays highlights the superior efficacy of OSR. This advantage can be attributed to OSR's strategy of directly transmitting packets to neighbouring nodes, eliminating potential inefficiencies associated with less direct paths or route discovery delays that might be encountered by the GRP protocols. At a distance of (8 km), OSR exhibits lower latency (min: 410 ms - max: 967 ms) compared to GRP-G (min: 810 ms - max: 1751 ms) and GRP-P (min: 770 ms - max 1600 ms). A traversal distance of (14 km) reveals a significant latency disparity. OSR exhibits lower latency (min: 693 ms - max: 1550 ms) compared to both GRP-G (min: 1500 ms - max: 2354 ms) and GRP-P (min: 1280 ms - max: 2134 ms) variants. These results underscore OSR's ability to minimize hop count and select the most efficient routing paths.

Table II highlights a trend where the OSR protocol often exhibits lower latency compared to GRP variants (GRP-G and GRP-P) as distance increases. Latency reduction may not scale directly with distance, as factors like resource allocation during congestion and CT challenges can significantly affect it.

Distance	Improvement over GRP-G	Improvement over GRP-P
1 Km	44.1%	30.5%
4 Km	63.5%	60.3%
8 Km	46.2%	41.9%
14 Km	41.8%	34.3%

TABLE II: Latency reductions of OSR versus GRP variants.

To assess the energy efficiency of our low-power mode OSR approach, we measured the total energy consumed by all devices when transmitting a set number of packets. The energy consumption parameters used in our study are as follows: a supply voltage of 3.3 V, a current of $28\,\mu$A in transmit mode (Tx), $11.2\,\mu$A in receive mode (Rx), $1.4\,\mu$A in standby mode, $0.0015\,\mu$A in sleep mode, and initial energy source (EI_{energy}) is $10,000$ joules. Under simultaneous data transmission from all EDs, the remaining energy level was 9988.2 joules of its initial $10,000$ joule energy allocation, indicating a minimal energy consumption of approximately 0.118%. Energy consumption was monitored across various time intervals: 0.98 joules over 2 hours, 2.95 joules over 6 hours, 5.9 joules over 12 hours, and 11.8 joules over 24 hours. This observed energy efficiency can be attributed to two key technical aspects of our OSR-DLM configuration: the used SF7 with a higher frequency modulation scheme [21], and the OSR sleep/wake-up cycles. Multiple simulations confirmed a linear relationship between energy consumption and time in the DLM network. This relationship was influenced by forwarding paths determined by the RCM and hop counts. OSR's ranking mechanism allocated time slots for routing decisions, with higher hop counts leading to increased routing activity and energy consumption. Despite the inactivity of some nodes, the overall energy consumption remained linearly proportional to time, demonstrating the efficiency of the low-power (LP) mode.

VI. Conclusions and future Works

This paper proposes Opportunistic Smart Routing (OSR), a novel multi-hop routing protocol specifically designed for LoRaWAN networks deployed in maritime environments. Extensive simulations demonstrate OSR's superior performance compared to traditional GRP variants, particularly in terms of PDR and end-to-end latency. OSR effectively addresses the challenges posed by maritime environments, including high packet loss and extended latency due to dynamic sea conditions and large operational ranges. The protocol achieves this by intelligently selecting routing paths with minimal hops and adaptively adjusting transmission strategies based on network conditions with low-power modes. This ensures robust and reliable data communication, which is critical for maritime operations. Future research could focus on addressing CT challenges within mesh networks, where efficient resource allocation could significantly improve PDR. Additionally, the practicality and adaptability of OSR can be further explored using the WisBlock modular system for real-world maritime deployments.

References

[1] F. S. Alqurashi, A. Trichili, N. Saeed, B. S. Ooi, and M.-S. Alouini, "Maritime communications: A survey on enabling technologies, opportunities, and challenges," IEEE Internet of Things Journal, vol. 10, no. 4, pp. 3525–3547, 2022.

[2] M. Alipio and M. Bures, "Current testing and performance evaluation methodologies of LoRa and LoRaWAN in IoT applications: Classification, issues, and future directives," Internet of Things, p. 101053, 2023.

[3] A. Osorio, M. Calle, J. D. Soto, and J. E. Candelo-Becerra, "Routing in LoRaWAN: Overview and challenges," IEEE Communications Magazine, vol. 58, no. 6, pp. 72–76, 2020.

[4] S. E. Elgharbi, M. Iturralde, Y. Dupuis, T. Coulombier, M. Menard, and A. Gaugue, "Multi-hop wireless transmission for maritime scenarios," in OCEANS 2023 - Limerick, 2023, pp. 1–10.

[5] C. E. Perkins and P. Bhagwat, "Highly dynamic destination-sequenced distance-vector routing (dsdv) for mobile computers," ACM SIGCOMM computer communication review, vol. 24, no. 4, pp. 234–244, 1994.

[6] B. Sartori, S. Thielemans, M. Bezunartea, A. Braeken, and K. Steenhaut, "Enabling rpl multihop communications based on LoRa," in 2017 IEEE 13th International Conference on Wireless and Mobile Computing, Networking and Communications (WiMob). IEEE, 2017, pp. 1–8.

[7] Y. Zhang, J. Luo, and H. Hu, Wireless mesh networking: architectures, protocols and standards. CRC Press, 2006.

[8] A. Hosseini-Fahraji, K. Zeng, Y. Yang, and M. Manteghi, "A self-sustaining maritime mesh network," in 2019 United States National Committee of URSI National Radio Science Meeting (USNC-URSI NRSM). IEEE, 2019, pp. 1–2.

[9] M. Msaad, A. Hambly, P. Mariani, and S. Kosta, "Mobile and delay tolerant network for LoRa at sea," in Proceedings of the Student Workshop, 2020, pp. 3–4.

[10] T. Patriti, S. Mirri, and R. Girau, "A LoRa-mesh based system for marine social IoT," in 2023 IEEE 20th Consumer Communications & Networking Conference (CCNC). IEEE, 2023, pp. 329–332.

[11] M. Bor, J. E. Vidler, and U. Roedig, "LoRa for the internet of things," 2016.

[12] J. Dias and A. Grilo, "LoRaWAN multi-hop uplink extension," Procedia Computer Science, vol. 130, pp. 424–431, 2018. [Online]. Available: https://www.sciencedirect.com/science/article/pii/S1877050918304216

[13] C. Ebi, F. Schaltegger, A. Rüst, and F. Blumensaat, "Synchronous LoRa mesh network to monitor processes in underground infrastructure," IEEE access, vol. 7, pp. 57 663–57 677, 2019.

[14] N. Le Sommer and L. Touseau, "Loraopp: A protocol for opportunistic networking and computing in LoRa networks," in 2022 18th International Conference on Wireless and Mobile Computing, Networking and Communications (WiMob). IEEE, 2022, pp. 308–313.

[15] L. Feng, H. Yu, and M. Jia, "A hierarchy-based dynamic routing protocol for LoRa mesh networks," in 2023 IEEE International Symposium on Broadband Multimedia Systems and Broadcasting (BMSB). IEEE, 2023, pp. 1–6.

[16] C. C. Chaguile, M. Alipio, and M. Bures, "A classification of cross-layer optimization approaches in LoRaWAN for internet of things," in 2023 Fourteenth International Conference on Ubiquitous and Future Networks (ICUFN). IEEE, 2023, pp. 259–264.

[17] K. P. Vijayakumar, P. Ganeshkumar, and M. Anandaraj, "Review on routing algorithms in wireless mesh networks," 2012. [Online]. Available: https://api.semanticscholar.org/CorpusID:18451233

[18] H. Kaur, H. Singh, and A. Sharma, "Geographic routing protocol: A review," International Journal of Grid and Distributed Computing, vol. 9, no. 2, pp. 245–254, 2016.

[19] M. Pandith, N. Ramaswamy, M. Srikantaswamy, and R. Ramaswamy, "A comprehensive review of geographic routing protocols in wireless sensor network," Inf. Dyn. Appl, vol. 1, no. 1, pp. 14–25, 2022.

[20] Nsnam, "ns-3 simulator," Available at: http://www.nsnam.org/, 2011.

[21] L. Casals, B. Mir, R. Vidal, and C. Gomez, "Modeling the energy performance of LoRaWAN," Sensors, vol. 17, no. 10, p. 2364, 2017.